

## XPS INVESTIGATION OF CERAMIC MATRIXES FOR DISPOSAL OF LONG-LIVING RADIOACTIVE WASTE PRODUCTS

by

**Yury A. TETERIN<sup>1</sup>, Serguei V. STEFANOVSKIJ<sup>2</sup>, Serguei V. YUDINTSEV<sup>3</sup>,  
George N. BEK-UZAROV<sup>4</sup>, Anton Yu. TETERIN<sup>1</sup>, Konstantin I. MASLAKOV<sup>1</sup>,  
and Igor O. UTKIN<sup>1</sup>**

Received on September 19, 2003; accepted on April 29, 2004

The synthesis of ceramic matrixes for the long-term storage of highly active radionuclide wastes and determination of physical and chemical forms of radionuclides in them is one of the important problems in radioecology. It enables to create purposefully materials for the long-term storage of radionuclides. In the present work the samples of ceramics [ $\text{CaCe}_{0.9}\text{Ti}_2\text{O}_{6.8}$  (I) and  $\text{CaCeTi}_2\text{O}_7$  (II)] formed under various conditions were investigated with the X-ray photoelectron spectroscopy. It is necessary for synthesis of ceramic matrixes, for the disposal of the plutonium and others tetravalent actinides. A technique was developed for the determination of cerium oxidation state ( $\text{Ce}^{3+}$  and  $\text{Ce}^{4+}$ ) on the basis of the X-ray photoelectron spectroscopy spectral structure characteristics. It was established that the sample (I) formed at 300 MPa and  $T = 1400^\circ\text{C}$  in the air atmosphere contained on the surface two types of cerium ions in the ratio – 63 atomic % of  $\text{Ce}^{3+}$  and 37 atomic % of  $\text{Ce}^{4+}$ , and the sample (II) formed at 300 MPa and  $T = 1300^\circ\text{C}$  in the oxygen atmosphere contained on its surface two types of cerium ions also, but in the ratio – 36 atomic % of  $\text{Ce}^{3+}$  and 64 atomic % of  $\text{Ce}^{4+}$ . It was established that on the surface of the studied ceramics carbonates of calcium and/or cerium could be formed under influence of the environment that leads to the destruction of ceramics.

*Key words: ceramics, matrix, XPS, cerium, radioactive wastes*

### INTRODUCTION

One of the most important ecological problems is a correct selection of ceramic matrixes for the long-term storage of long-lived radionuclides and high-level wastes (HLW). An understanding and prediction of chemical processes in such ceramic matrixes requires the knowledge of physical

and chemical states of radionuclides and elements of ceramic matrixes (elemental and ionic composition, oxidation states, number of uncoupled electrons in ions, chemical bond nature, structure of close environment, *etc.*). This would enable production of purposeful materials for the long-term storage of the HLW and actinide wastes of various compositions. Determination of oxidation states of elements in HLW ceramics can be achieved by, for example, XANES [1, 2] and EPR [3, 4]. One of the most adequate methods of determination of the state of radionuclides in environment is X-ray photoelectron spectroscopy (XPS) [5, 6].

The present work carried out the XPS study of ceramics of the calculated compositions  $\text{CaCe}_{0.9}\text{Ti}_2\text{O}_{6.8}$  (I) and  $\text{CaCeTi}_2\text{O}_7$  (II) produced under various conditions, which are the model materials in production of the ceramic matrixes for immobilization of plutonium and other tetravalent actinides. One of the main goals was to develop a technique of cerium oxidation state determination on the basis of the

Scientific paper

UDC: 666.3.017:546.655:681.785.5

BIBLID: 1451-3994, 19 (2004), 1, pp. 31-38

Authors' addresses:

<sup>1</sup> Russian Research Center "Kurchatov Institute"

1, Kurchatov sq., Moscow 123182, Russia

<sup>2</sup> NPO "Radon", 2/14, 7 Rostovsky st.,

Moscow 119121, Russia

<sup>3</sup> Institute of Geology of Ore Deposits of RAS,  
35, Staromonetny st., Moscow 119017, Russia

<sup>4</sup> VINČA Institute of Nuclear Sciences

P. O. Box 522, 11001 Belgrade, Serbia and Montenegro

E-mail address of corresponding author:  
teterin@ignph.kiac.ru (Y. A. Teterin)

fine XPS structure parameters. The traditional information (binding energies, line intensities and chemical shifts) are not sufficient for the determination of cerium oxidation states because of the spectral structure complication [6-8]. So, to determine cerium oxidation state in compounds, the present work used the fine core and outer XPS structure parameters.

## EXPERIMENTAL

Samples of the calculated compositions  $\text{CaCe}_{0.9}\text{Ti}_2\text{O}_{6.8}$  (I) and  $\text{CaCeTi}_2\text{O}_7$  (II) were prepared from the mixtures of  $\text{CaCO}_3$ ,  $\text{CeO}_2$ , and  $\text{TiO}_2$  ground in the agate mortar to the size of 20–30  $\mu\text{m}$ . The mixtures were pressed at 300 MPa into tablets of 20 mm in diameter and 3 mm high and sintered at 1400 °C in the air (Sample I) and at 1300 °C in oxygen (Sample II) for 20 hours. Preliminary parameters of the samples are given in [9]. More detailed data were measured with X-ray diffractometer DRON-4 ( $\text{Cu K}\alpha$  – irradiation) and scanning electron microscope with the energy dispersion system (SEM-EDS) on the analytical complex JSM-5300 + Link ISIS.

XPS spectra of the studied solid-state samples were taken with an HP-5950A spectrometer using monochromatized  $\text{Al K}\alpha_{1,2}$  ( $h\nu = 1486.6 \text{ eV}$ ) X-rays (Compounds 3-7, tab. 1) and MK II VG Scientific (Compounds 1 and 2, tab. 1) at  $\sim 1.3 \cdot 10^{-7} \text{ Pa}$  at room temperature. Overall resolution measured as the  $\text{Au } 4f_{7/2}$  electron line full width half maximum (FWHM) was better than 0.8 eV (IE 5950A) and 1.2 eV (IE II VG Scientific). Electron binding energies are given relative to the  $E_b$  of (C1s) electrons from adventitious hydrocarbons at the sample surface defined as 285.0 eV. The measurement errors of line position and widths were 0.1 eV, whereas relative line intensities errors were about 10%. The sample materials were prepared by pressing powders into indium on titanium substrates.

The quantitative atomic and elemental analysis based on the fact that the peak intensities are proportional to the ionic concentration was done for all the studied samples. It was done using the ratio:  $n_i/n_j = (S_i/S_j)(k_j/k_i)$ , where  $n_i/n_j$  is the relative concentration of the studied atoms,  $S_i/S_j$  – relative intensity (area) of the corresponding core XPS lines, and  $k_j/k_i$  – experimental relative sensitivity coefficient. This work used the following coefficient relative to carbon: 1.00 (C1s); 2.8 (O1s); 4.8 ( $\text{Ti } 2p_{3/2}$ ); 4.2 ( $\text{Ca } 2p_{3/2}$ ), and 20.3 ( $\text{Ce } 3d_{5/2}$ ). Sensitivity coefficient  $k_i(\text{Ce } 3d_{5/2}) = 20.3$  for  $\text{Ce } 3d_{5/2}$  was found for  $\text{CeNbO}_4$  taking into account the corresponding  $k_j(\text{Nb } 3d) = 9.6$  for the Nb3d electrons. The spectral parameters of  $\text{CeO}_2$ ,  $\text{CeNbO}_4$ ,  $\text{CeL}_3$ ,

and  $\text{CeL}_3' \cdot 1.5\text{H}_2\text{O}$ , where L – and L' – residua of ortho-metoxibenzoic [ $\text{CH}_3\text{OC}_6\text{H}_4\text{COO}^-$ ] and diphenyl-acetic [ $(\text{C}_6\text{H}_5)_2\text{CHCOO}^-$ ] acids, were used for interpretation of the XPS spectra from the studied samples (Samples I and II).

## RESULTS AND DISCUSSION

As it follows from the diffractograms (fig. 1), Sample I was formed mostly by the perovskite-based phase (~85%) and a small amount of cerianite (~15%). By the SEM-EDS data, the chemical composition of the general mass changes slightly in the sample bulk. Against the background of the general perovskite-related mass,  $(\text{Ca}_{0.56}\text{Ce}_{0.32}\text{Ti}_{0.98}\text{O}_3)$  dark on the SEM image (fig. 2a), some lighter grains were observed (fig. 2b). They consist of pyrochlorite  $(\text{Ca}_{1.08}\text{Ce}_{0.89}\text{Ti}_{2.03}\text{O}_{6.92})$  with 4 cations. Sample I contains not more than ~3% of this phase, since it could not be detected by the X-ray diffraction. Perovskite formula in this case corresponds to the solid solution  $\text{CaTiO}_3\text{--Ce}_{0.66}\text{TiO}_{2.975}$ . Cerianite formula is  $\text{Ce}_{0.94}\text{Ti}_{0.04}\text{Ca}_{0.02}\text{O}_{1.97}$ .

Sample II was based on pyrochlorite, whose contents was 70–80% (fig. 1b). This phase is manifested in the SEM image (fig. 2c) as gray mass, while the impurity perovskite phases (the darker spots) and cerianite phase (white grains) took 10–15% each. The SEM-EDS data show that these phases correspond to formulas  $\text{Ca}_{1.06}\text{Ce}_{0.98}\text{Ti}_{1.96}\text{O}_{6.94}$ ,  $\text{Ca}_{0.80}\text{Ce}_{0.18}\text{Ti}_{0.95}\text{O}_3$ , and  $\text{Ce}_{0.92}\text{Ti}_{0.06}\text{Ca}_{0.02}\text{O}_{1.98}$ , respectively.

The technique of determination of physical and chemical states of elements in the studied cerium compounds used in this work is based on both traditional XPS parameters (electron binding energies and line intensities) and fine core and outer spectral structure parameters such as: relative intensity of the Ce4f electrons weakly participating in the chemical bond, relative binding energies of the inner valence molecular orbitals (IVMO), core line multiplet splitting, fine spectral structure parameters due to the dynamic effect, relative binding energies of shake up satellites in the core level spectra [5, 6]. These spectral data provide much information on the physical and chemical states of lanthanides, in particular – cerium, in compounds [7, 8].

**Low binding energy spectral range.** Since atomic cerium electronic configuration is  $\{\text{Xe } 4f^1 5d^1 6s^2, \text{Ce}^{3+} - \{\text{Xe}\} 4f^1, \text{ and } \text{Ce}^{4+} - \{\text{Xe}\} 4f^0$ , where  $\{\text{Xe}\}$  xenon electronic configuration, XPS spectra from  $\text{Ce}^{3+}$  compounds unlike those from  $\text{Ce}^{4+}$  ones are expected to manifest the line related to the localized Ce4f electrons for the basic  $\text{Ce}^{3+}$  state around zero binding energy. Indeed, this line shows up in the XPS spectra

Figure 1. Diffractograms of ceramic samples: (a) –  $\text{CaCe}_{0.9}\text{Ti}_2\text{O}_{6.8}$  (I); (b) –  $\text{CaCeTi}_2\text{O}_7$  (II); C – cerianite, P – perovskite, Py – pyrochlorite

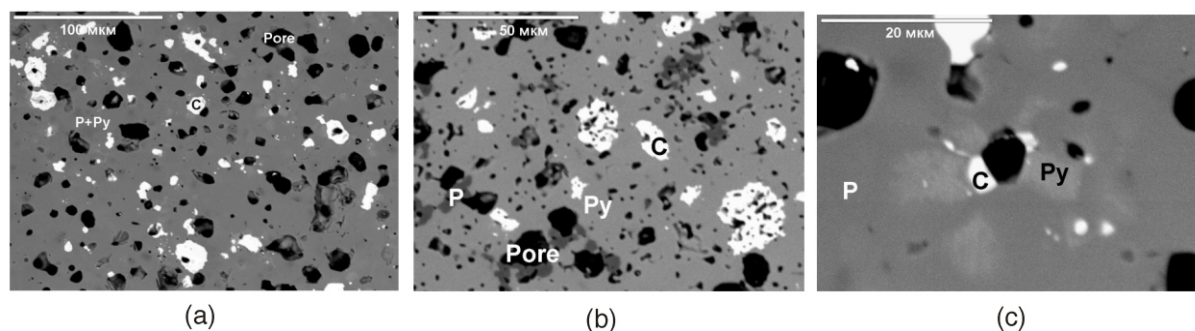
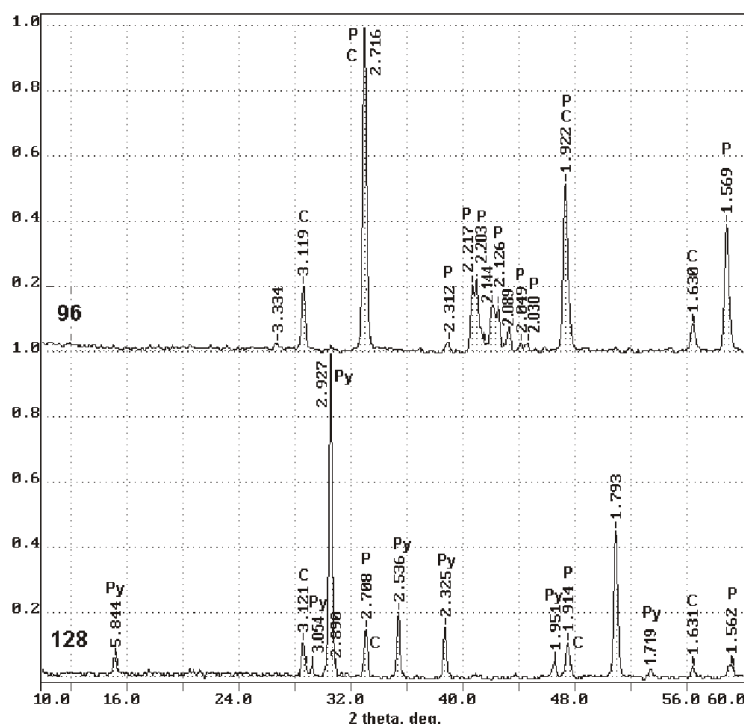


Figure 2. Scanning electron microscope images of ceramic samples: (a, b) –  $\text{CaCe}_{0.9}\text{Ti}_2\text{O}_{6.8}$  (I); (c) –  $\text{CaCeTi}_2\text{O}_7$  (II). In figures (a), (b), and (c) the MKM symbol denotes micrometer

from  $\text{CeF}_3$ ,  $\text{CeNbO}_4$ ,  $\text{CeL}_3$ , and  $\text{CeL}_3 \cdot 1.5\text{H}_2\text{O}$  and does not show up in the spectra from  $\text{CeO}_2$  [6, 10]. The relative intensity of this line measured as the ratio  $\text{Ce}4f/\text{Ce}5s$  line areas is  $0.61 \pm 0.03$ ,  $0.38 \pm 0.04$ , and  $0.41 \pm 0.04$  for  $\text{CeF}_3$ ,  $\text{CeL}_3$ , and  $\text{CeL}_3 \cdot 1.5\text{H}_2\text{O}$ , which corresponds to the electronic densities  $1.00 \pm 0.05$ ,  $0.77 \pm 0.08$ , and  $0.84 \pm 0.08e^-$  respectively [7, 8]. The low binding energy XPS spectrum indicates that Sample I can contain an admixture of  $\text{Ce}^{3+}$  ions since a low intense  $\text{Ce}4f$  related peak is observed around zero binding energy (at  $\sim 2$  eV) (fig. 3c). Unfortunately, this spectrum does not allow a correct quantitative evaluation of the  $\text{Ce}4f$  intensity since the  $\text{Ce}5s$  is overlapped with the intense  $\text{Ti}3p$  line and the other Ce lines are structured and the sample contains cerium ions of different oxidation states (fig. 3c). Beside the band in the binding energy range 0-10 eV, due to the outer

valence molecular orbitals (OVMO), the XPS spectrum shows the structure due to the inner valence molecular orbitals (OVMO) in the binding energy range 10-45 eV. These IVMOs are related to the  $\text{Ce}5s, 5p$ ,  $\text{Ca}3s, 3p$ ,  $\text{Ti}3p$  and  $\text{O}2s$  atomic orbitals (AO) from the neighboring atoms [6, 10]. The binding energies for Samples I and II are qualitatively comparable to each other and other  $\text{Ce}^{3+}$  and  $\text{Ce}^{4+}$  containing compounds (tab. 1).

**Core electron spectral range.** During sample preparation some hydrocarbon and water molecules may absorb on the sample surfaces. The existing techniques of surface cleaning were not used in the present work in order to avoid sample destruction. The C1s spectra show the peaks at  $E_b = 285.0$  eV (saturated hydrocarbons) used for the binding energy calibration, and  $\text{CO}_3^{2-}$  related peaks at  $E_b = 288.5$  eV (fig. 4). The spec-

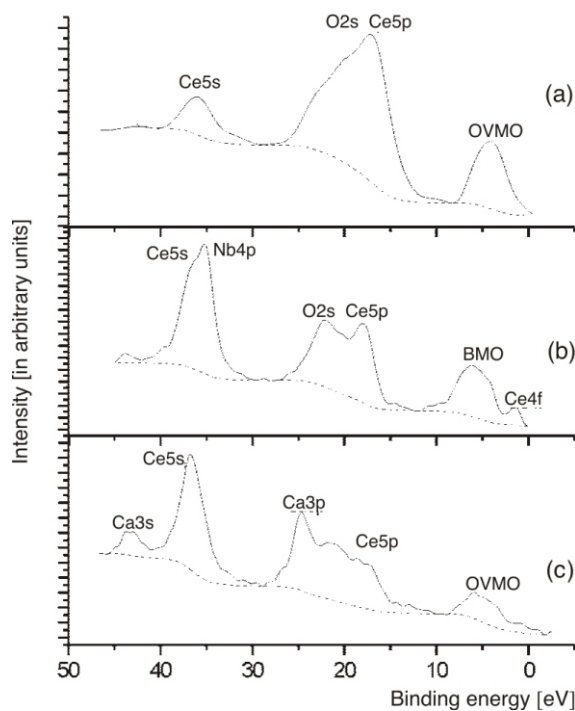


Figure 3. Low binding energy XPS spectra from: (a) –  $\text{CeO}_2$ , (b) –  $\text{LnNbO}_4$ , (c) –  $\text{CaCe}_{0.9}\text{Ti}_2\text{O}_{6.8}$  (I). Spectral intensity was no normalized

trum from Sample I shows an extra low intense peak at  $E_b = 280.3$  eV which was attributed to metal carbides (fig. 4a). The O1s spectra show the basic lines at  $E_b = 529.5$  eV and extra lines at about  $E_b = 532$  eV attributed to oxygen of carbonate group and water (fig. 5). Despite the surface contamination, their XPS lines were observed, intense and sharp. Thus, the  $\text{Ti}2p_{3/2}$  binding energy (Sample II)  $E_b = 458.2$  eV agrees to the corresponding binding energy for

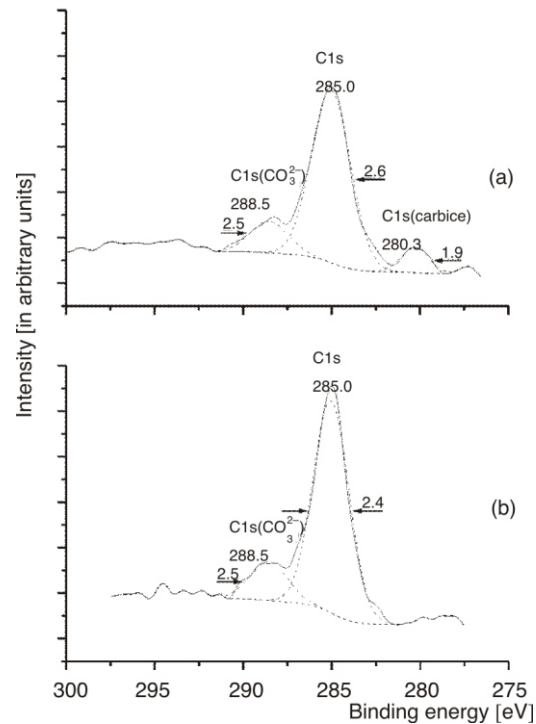


Figure 4. C1s XPS spectra from: (a) –  $\text{CaCe}_{0.9}\text{Ti}_2\text{O}_7$  (I), (b) –  $\text{CaCeTi}_2\text{O}_7$  (II). Spectral intensity was no normalized

$\text{La}_2\text{Ti}_2\text{O}_7$  458.4 eV and to a lesser degree – to 459.0 eV for  $\text{TiO}_2$  [10]. This spectrum shows the typical shake up satellites (fig. 6). The  $\text{Ca}2p$  spectra from the studied samples show low intense shake up satellites, and the  $\text{Ca}2p_{3/2}$  binding energy  $E_b = 346.5$  eV (fig. 7) differs from that for  $\text{CaO}$  346.0 eV [11].

**Ce3d XPS spectra.** The most intense cerium line is the Ce3d one. For metallic cerium this line consists of a spin-orbit interaction related doublet

Table 1. Core and outer electron binding energies ( $E_b^{(a)}$ , eV) of samples (I, II) and cerium compounds [6, 10]

| N | Compound  | Ion              | OVMO               |                    | IVMO                |           |           | Core levels                        |        |
|---|---|------------------|--------------------|--------------------|---------------------|-----------|-----------|------------------------------------|--------|
|   |   |                  | Ce4f               | Ce5d, 6s<br>O(F)2p | Ce5p <sub>3/2</sub> | O(F)2s    | Ce5s      | Ce3d <sub>5/2</sub> <sup>(b)</sup> | O(F)1s |
| 1 | $\text{CaCe}_{0.9}\text{Ti}_2\text{O}_{6.8}$ (I) <sup>(c)</sup> |                  | 1.2 <sup>(c)</sup> | 5.0                | 17.7                | 21.2      |           | (882.8) 884.8                      | 529.5  |
| 2 | $\text{CaCeTi}_2\text{O}_7$ (II) <sup>(d)</sup>                 |                  |                    |                    |                     |           |           | 882.6 (889.1) 898.6                | 529.5  |
| 3 | $\text{CeO}_2$  | $\text{Ce}^{4+}$ |                    | 5.0                | 18.0                |           | 36.8      | 882.3 (888.8) 898.0                | 529.5  |
| 4 | $\text{CeNbO}_4$  | $\text{Ce}^{3+}$ | 1.4                | 5.8                | 17.8                | 21.8      |           | (881.8) 885.8                      | 530.0  |
| 5 | $\text{CeL}_3$  | $\text{Ce}^{3+}$ | 2.2                | 5.1                | 18.7                | 25.7 27.0 | 37.3 38.3 | (882.8) 885.8                      | 531.8  |
| 6 | $\text{CeL}'_3 \cdot 1.5\text{H}_2\text{O}$                     | $\text{Ce}^{3+}$ | 3.2                | 5.8                | 19.3                | 25.8      | 37.3      | (882.3) 885.4                      | 532.4  |
| 7 | $\text{CeF}_3$  | $\text{Ce}^{3+}$ | 3.4                | 8.4                | 19.4                | 29.5      | 38.0      | 884.7 (888.2)                      | 685.4  |

<sup>(a)</sup> Binding energies given for the peak maxima, in cases when the atomic lines of Ln, Nb, and O overlap, the binding energies are not given in the table

<sup>(b)</sup> Parameters of less intense of the two neighbouring peaks belonging to the common structure are given in parenthesis

<sup>(c)</sup> Contains 0.63 of  $\text{Ce}^{3+}$  ions and 0.37 of  $\text{Ce}^{4+}$  ions

<sup>(d)</sup> Contains 0.36 of  $\text{Ce}^{3+}$  ions and 0.64 of  $\text{Ce}^{4+}$  ions

<sup>(e)</sup> Low intense line



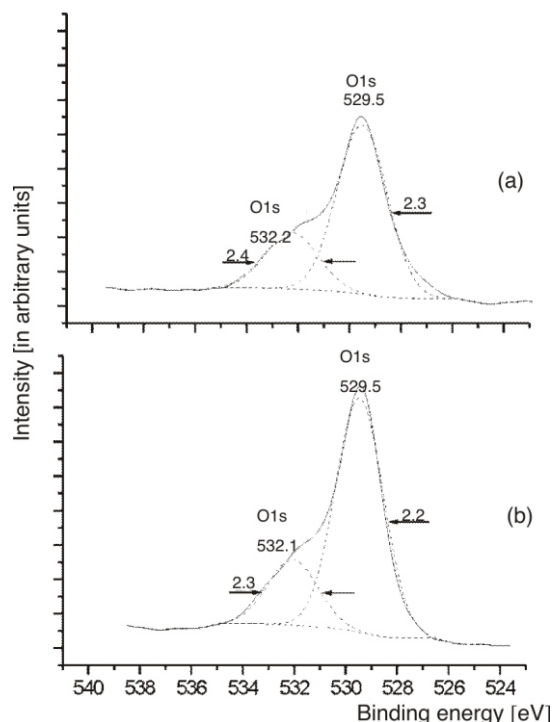


Figure 5. O1s XPS spectra from: (a) –  $\text{CaCe}_{0.9}\text{Ti}_2\text{O}_7$  (I), (b) –  $\text{CaCeTi}_2\text{O}_7$  (II). Spectral intensity was no normalized

with the splitting  $E_{so}(\text{Ce}3d) = 18.5$  eV [12]. Beside the basic lines, this spectrum shows the many-body perturbation related shake up satellite on the higher binding energy side. The structures of these satellites are typical for certain oxygen-containing cerium compounds. Thus, the Ce3d spectral structure for  $\text{Ce}^{3+}$  compounds is well known [6, 10]. For example, for  $\text{CeNbO}_4$  this structure consists of a spin-orbit doublet with the splitting  $E_{so}(\text{Ce}3d) = 18.3$  eV and intense ( $I_s/I_0 = 113\%$ ) shake up satellites at 3.8 eV on the higher binding energy side from the basic lines (fig. 8b). The Ce3d spectrum for  $\text{CeO}_2$  containing  $\text{Ce}^{4+}$  ions beside the basic spin-doublet shows some extra peaks [13], which are absent in the corresponding spectra from  $\text{Ce}^{3+}$  oxygen containing compounds and cerium trifluoride (fig. 8a, tab. 1). The considered extra structure at  $E_b = 898.0$  eV (tab. 1) and  $E_b = 916.3$  eV for  $\text{CeO}_2$  is a 18.3 eV split doublet. This splitting agrees well with the observed in this work Ce3d splitting  $E_{so}(\text{Ce}3d) = 18.3$  eV and the data of [14]. Such a fine spectral structure was suggested in [7, 8] to be due to the unusual final state of cerium ions after the photoemission of a Ce3d electron.

This final state can be the result of the many-body perturbation (shake up process) with the transfer of a Ce5s (or Ce5p) electron to the vacant molecular orbitals (MO) during the Ce3d photoemission. As a result, an extra quasi-core hole in

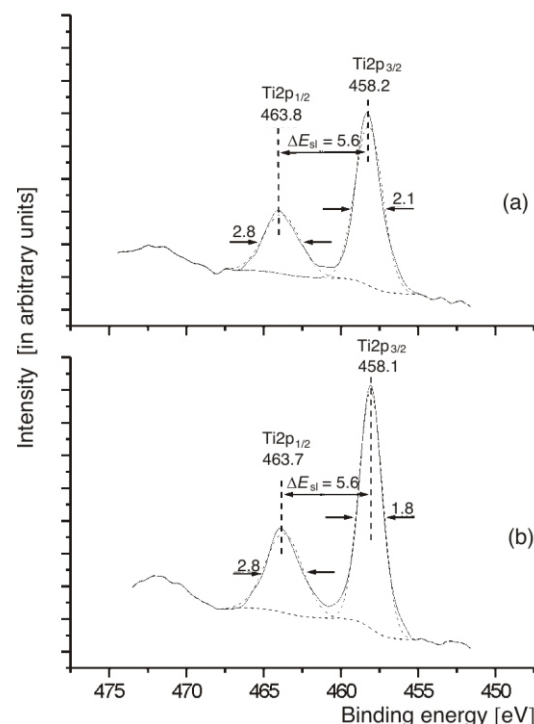


Figure 6. Ti2p XPS spectra from: (a) –  $\text{CaCe}_{0.9}\text{Ti}_2\text{O}_7$  (I), (b) –  $\text{CaCeTi}_2\text{O}_7$  (II). Spectral intensity was no normalized

the Ce5s(5p) forms, which is responsible for the final state  $\text{Ce}3d^9 5s^1 4f^0 \text{MO}^{n+1}$  (or  $\text{Ce}3d^9 5p^5 4f^0 \text{MO}^{n+1}$ ) shifted in relation to the basic final state by 15.7 eV.

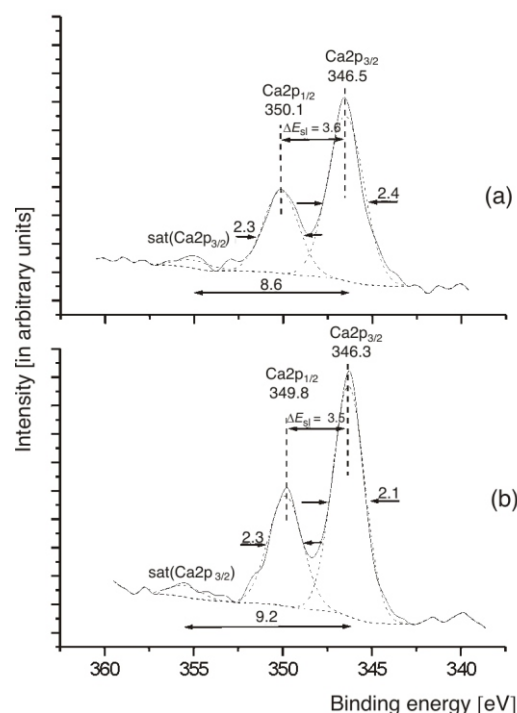
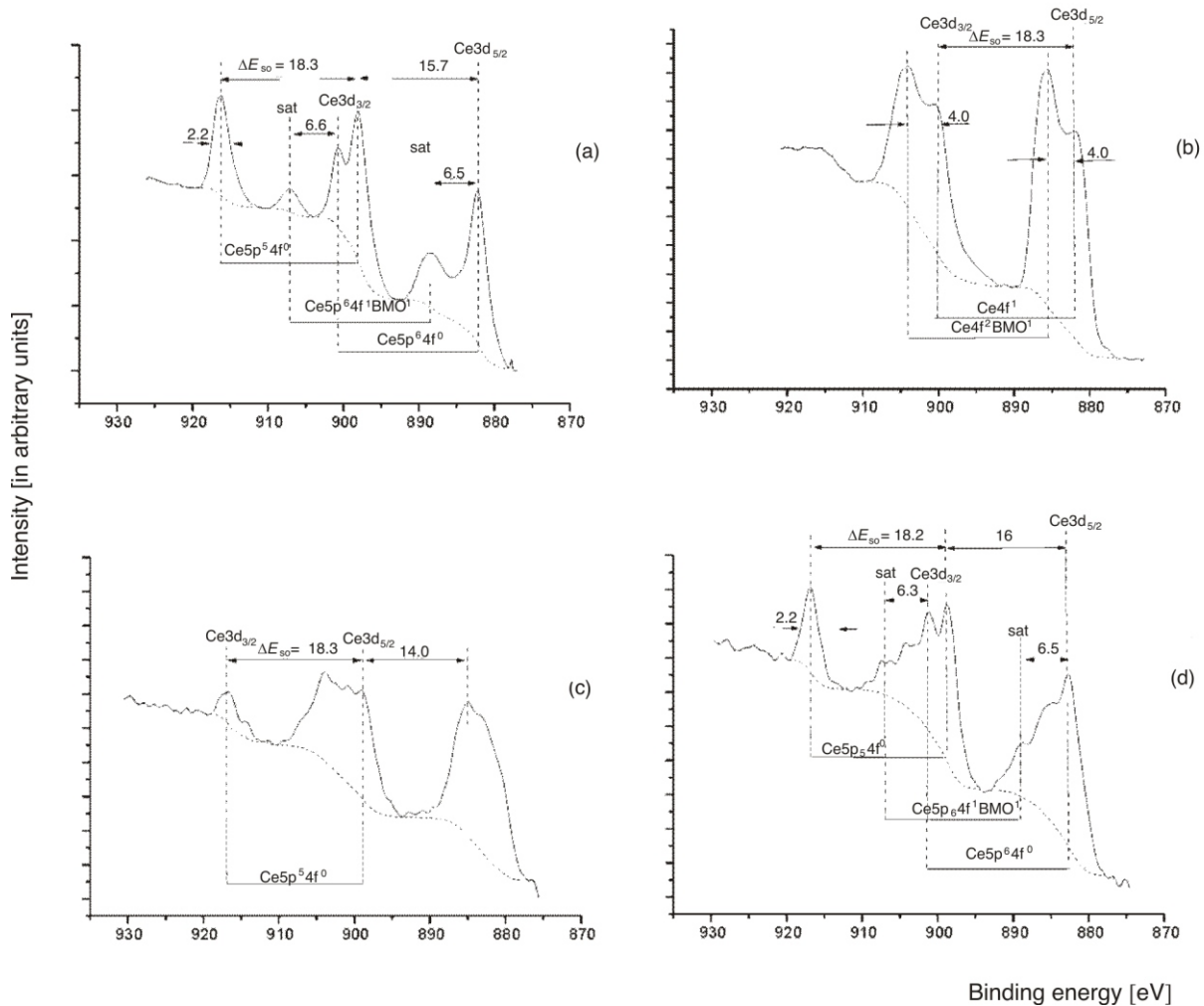


Figure 7. Ca2p XPS spectra from: (a) –  $\text{CaCe}_{0.9}\text{Ti}_2\text{O}_7$  (I); (b) –  $\text{CaCeTi}_2\text{O}_7$  (II). Spectral intensity was no normalized



**Figure 8.** Ce3d XPS spectra from: (a) – CeO, (b) – LnNbO<sub>4</sub>; (c) – CaCe<sub>0.9</sub>Ti<sub>2</sub>O<sub>7</sub> (I); (d) – CaCeTi<sub>2</sub>O<sub>7</sub> (II). Spectral intensity was no normalized

This agrees with the calculation results of the work [14], which suggested that during the Ce3d photoemission, a complex final state is established, consisting of three states Ce3d<sup>9</sup>4f<sup>0</sup> (882.3 and 900.6 eV), Ce3d<sup>9</sup>4f<sup>1</sup>OVMO<sup>-1</sup> (888.8 and 907.2 eV), and Ce3d<sup>9</sup>5p<sup>5</sup>np (898.0 and 916.3 eV). In the Ce3d three doublets correspond to these final states (fig. 8a, tab. 1). The probabilities of these final states proportional to the areas of the corresponding spectral lines found from the Ce3d spectra of CeO<sub>2</sub> (fig. 8a) are:  $0.43 \pm 0.08$  (Ce3d<sup>9</sup>4f<sup>0</sup>),  $0.21 \pm 0.04$  (Ce3d<sup>9</sup>4f<sup>1</sup>OVMO<sup>-1</sup>), and  $0.36 \pm 0.04$  (Ce3d<sup>9</sup>5p<sup>5</sup>np).

The Ce3d XPS spectrum from CeNbO<sub>4</sub> containing Ce<sup>3+</sup> ions (fig. 8b) corresponds well to the spectra from other trivalent cerium compounds (tab. 1), in particular, Ce<sub>2</sub>O<sub>3</sub> [15]. The structure of this spectrum is due to the complex final state consisting of the two states Ce3d<sup>9</sup>4f<sup>1</sup> (881.8 and 900.1 eV) and Ce3d<sup>9</sup>4f<sup>2</sup>OVMO<sup>-1</sup> (885.8 and 904.1 eV) (fig. 8b).

Despite the fact that the Ce3d XPS spectrum from Sample I is by its structure close to that of CeNbO<sub>4</sub>, and the one from Sample II – to that of CeO<sub>2</sub>, these spectra still reflect the complex phases of the studied compounds (Fig. 8c, d). However, having suggested that Samples I and II contain formally Ce<sup>3+</sup> and Ce<sup>4+</sup> ions, one can evaluate the relative percent ionic compositions of these compounds using the areas of low energy (Ce3d<sub>5/2</sub> at  $E_b = 885$  eV) and high energy (Ce3d<sub>3/2</sub> at  $E_b = 916$  eV) components  $S_1$  and  $S_0$  (fig. 8). Indeed, since the area ratio in the spectrum from CeO<sub>2</sub> can easily be determined by using the photoionization cross-sections, one can subtract the Ce<sup>4+</sup> related area from the total Ce3d area for the studied samples. Having suggested that the remaining area corresponds to Ce<sup>3+</sup>, it is possible to determine the quantitative ionic composition. In practice only the Ce3d<sub>5/2</sub> lines were used that simplifies this determination. If the ratio of the Ce3d<sub>5/2</sub> components  $S_1$  and  $(3/2)S_0$  for CeO<sub>2</sub> is already

known to be  $a = S_1/(3/2)S_0$ , the parts  $\nu(\text{Ce}^{3+})$  and  $\nu(\text{Ce}^{4+})$  in the studied sample are:

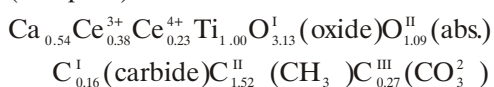
$$\nu(\text{Ce}^{3+}) = \frac{1 - a \frac{3S_0}{2S_1}}{1 - \frac{3S_0}{2S_1}} \quad (1)$$

$$\nu(\text{Ce}^{4+}) = 1 - \nu(\text{Ce}^{3+}) \quad (2)$$

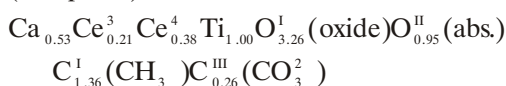
In this approximation using eqs. (1) and (2) the  $\text{Ce}^{3+}$  and  $\text{Ce}^{4+}$  concentrations were found to be  $\nu(\text{Ce}^{3+}) = 0.63$  and  $\nu(\text{Ce}^{4+}) = 0.37$  for Sample I, and  $\nu(\text{Ce}^{3+}) = 0.36$  and  $\nu(\text{Ce}^{4+}) = 0.64$  for Sample II. These data reflect the stoichiometric surface compositions of crystalline and amorphous fractions and can differ from the X-ray diffraction data. However, these ratios agree well with the X-ray diffraction and SEM-EDS data. Thus, in Sample I perovskite structure containing  $\text{Ce}^{3+}$  prevails, and the extra structure is cerianite related with  $\text{Ce}^{4+}$ . Beside, the sample contains an impurity pyrochlorite like phase with tetravalent cerium. In Sample II the main phase is pyrochlorite containing  $\text{Ce}^{4+}$ , with the extra ones of cerianite with  $\text{Ce}^{4+}$  and perovskite with  $\text{Ce}^{3+}$ .

An extra error in quantitative elemental and ionic chemical analysis of the studied samples (Samples I, II) comes from the complex fine spectral structure due to the secondary electronic processes (many-body perturbation and dynamic effect). It complicates the correct measurement of spectral line areas. Since the many-body perturbation results in the shake up satellites on the higher binding energy side from the basic lines, their intensities can be partially taken into account in the quantitative analysis (fig. 6-8). To take into account the influence of the dynamic effect is difficult, but its influence on the considered spectra is not high. It all can cause an error of more than 10% in the quantitative analysis. In this approximation the surfaces of the studied samples were found to have the following compositions relative to titanium atoms:

(Sample I)



(Sample II)



where the value 1.09 for oxygen  $\text{O}^{\text{II}}$  (Sample I) can include 0.81 of oxygen from  $(\text{CO}_3^2)$ , 0.27 of

oxygen from the basic oxides. The value 0.95 for oxygen  $\text{O}^{\text{II}}$  (Sample II) can include 0.78 of oxygen from  $(\text{CO}_3^2)$ , 0.17 of oxygen from the basic oxides. Since the oxygen concentration was measured more correctly, one can conclude that the extra surface oxygen is included in the carbonate groups connected with calcium and/or cerium. From the practice of the XPS study of HTSC metal-oxide ceramics calcium is known to form actively carbonates on the surface [6]. With this in mind, excluding the impurity carbon compounds except for carbonates on the sample surface, the following formulas can be written for the surface stoichiometric compositions:

(Sample I)



(Sample II)



where carbonate groups can be connected with both calcium and cerium. It has to be noted that calcium and cerium contents in the samples was slightly overestimated due to the measurement error, as it was discussed earlier in this work. Despite this and the fact that the present data were obtained for the surface of the studied samples, the XPS data coincide with the X-ray diffraction and electron microscopy results (fig. 1, 2, and text).

## CONCLUSIONS

On the basis of cerium fine core and outer X-ray photoelectron spectral data a technique of determination of cerium oxidation state, relative ionic composition of  $\text{Ce}^{3+}$  and  $\text{Ce}^{4+}$  containing compounds was developed. It enabled analysis of two samples of calcium-cerium-titanium ceramics [ $\text{CaCe}_{0.9}\text{Ti}_2\text{O}_{6.8}$  (I) and  $\text{CaCeTi}_2\text{O}_7$  (II)], which are the matrixes for the long-term storage of the long-lived radionuclides and high-level wastes.

Sample I produced at 300 MPa and 1400 °C in the air was found to contain on its surface two types of cerium ions in the ratio 63 at.% of  $\text{Ce}^{3+}$  and 37 at.% of  $\text{Ce}^{4+}$ . Sample II produced at 300 MPa and 1300 °C in oxygen, contained also two types of cerium ions in the ratio 36 at.% of  $\text{Ce}^{3+}$  and 64 at.% of  $\text{Ce}^{4+}$ . This agrees satisfactorily with the data of X-ray diffraction analysis and scanning electron microscopy.

The interaction with the environment was shown to result in formation of calcium and/or cerium carbonates on ceramics surface. It can lead to destruction of ceramics.

## ACKNOWLEDGEMENTS

The work was financially supported by the RFBR grant N 02-03-32693a, ISTC grant N 1358 and State program Leading scientific schools, grant N 1763.

## REFERENCES

- [1] Begg, B. D., Vance, E. R., Day, R. A., Hambley, M., Conradson, S. D., Plutonium and Neptunium Incorporation in Zirconolite, *Mat. Res. Soc. Symp. Proc.*, 465 (1997), pp. 325-332
- [2] Begg, B. D., Vance, E. R., The Incorporation of Cerium in Zirconolite, *Mat. Res. Soc. Symp. Proc.*, 465 (1997), pp. 333-340
- [3] Sobolev, I. A., Stefanovsky, S. V., Lifanov, F. A., Synthetic Melted Rock-Type Wasterforms, *Mat. Res. Soc. Symp. Proc.*, 333 (1995), pp. 833-840
- [4] Begg, B. D., Vance, E. R., Lumpkin, G. R., Charge Compensation and the Incorporation of Cerium in Zirconolite and Perovskite, *Mat. Res. Soc. Symp. Proc.*, 506 (1998), pp. 79-86
- [5] Teterin, Yu. A., Gagarin, S. G., Inner Valence Molecular Orbitals and the Structure of X-Ray Photoelectron Spectra, *Russian Chemical Reviews.*, 65 (1996), 10, pp. 825-847
- [6] Teterin, Yu. A., Teterin, A. Yu., Structure of X-Ray Photoelectron Spectra of Lanthanide Compounds, *Russian Chemical Reviews.*, 71 (2002), 5, pp. 347-381
- [7] Teterin, Yu. A., Teterin, A. Yu., Lebedev, A. M., Utkin, I. O., The XPS Spectra of Cerium Compounds Containing Oxygen, *J. Electron. Spectrosc. Relat. Phenom.*, 88-91 (1998), pp. 275-279
- [8] Teterin, Yu. A., Teterin, A. Yu., Lebedev, A. M., Utkin, I. O., Structure of X-Ray Photoelectron Spectra of Cerium Compounds Containing Oxygen (in Russian), *Radiohimiya*, 40 (1998), 2, pp. 97-102
- [9] Yudintsev, S. V., Stefanovsky, S. V., Jung, Ya. N., Che, S., Investigation by the Method of X-Ray Diffraction of Formation of Phases at Synthesis of Matrixes for Actinides (in Russian), *Steklo i Keramika*, 7 (2002), pp. 18-22
- [10] Teterin, Yu. A., Baev, A. S., X-Ray Photoelectron Spectroscopy of Lanthanide Compounds (in Russian), TsNII Atominform, Moscow, 1987, p.128
- [11] Sosulnikov, M. I., Teterin, Yu. A., X-Ray Photoelectron Studies of Ca, Sr, Ba and their Oxides and Carbonates, *J. Electron. Spectrosc. Relat. Phenom.*, 59 (1992), pp. 111-126
- [12] Praline, G., Koel, B. E., Hance, R. L., Lee, H.-I., Waite, J. M., X-Ray Photoelectron Study of the Reaction of Oxygen with Cerium, *J. Electron. Spectrosc. Relat. Phen.*, 21 (1980), pp. 17-30
- [13] Kaindl, G., Wertheim, G. K., Schmiester, G., Sampathkumaran, E. V., Mixed Valency Versus in Rare-Earth Core-Electron Spectroscopy, *Phys. Rev. Letters.*, 58 (1987), 6, pp. 606-609
- [14] Thornton, G., Dempsey, M. J., Final-State Effects in the 3d and 4d X-Ray Photoelectron Spectra of CeO<sub>2</sub>, *Chem. Rev. Lett.*, 77 (1981), 2, pp. 409-412
- [15] Fuggle, J. C., Campagna, M., Zolnierrek, Z., Lasser, R., Observation of a Relationship between Core-Level Line Shapes in Photoelectron Spectroscopy and Localization of Screening orbitals, *Phys. Rev. Letters.*, 45 (1980), 19, pp. 1597-1600

**Јуриј А. ТЕТЕРИН, Сергеј В. СТЕФАНОВСКИЈ, Сергеј В. ЈУДИНЦЕВ,  
Ђорђе Н. БЕК-УЗАРОВ, Антон Ју. ТЕТЕРИН, Константин И. МАСЛАКОВ, Игор О. УТКИН**

**ПРОУЧАВАЊЕ КЕРАМИЧКИХ МАТРИЦА ЗА ОДЛАГАЊЕ  
ДУГОЖИВЕЋЕГ РАДИОАКТИВНОГ ОТПАДА XPS ПОСТУПКОМ**

Синтеза керамичких матрица за трајно смештање радиоактивног отпада високе активности и одређивање физичких и хемијских форми радионуклида у њима, један је од значајних задатака радиоекологије јер омогућава да се створе сврсисходни материјали за ове потребе. У овом раду, керамички узорци [CaCe<sub>0.9</sub>Ti<sub>2</sub>O<sub>6.8</sub> (I) и CaCeTi<sub>2</sub>O<sub>7</sub> (II)] обликовани под различитим условима проучавани су рендгенском фотоелектронском спектроскопијом у циљу синтезе керамичких матрица за потребе одлагања плутонијума и других тетравалентних актинида. Развијена је посебна техника за одређивање церијумовог оксидационог стања (Ce<sup>3+</sup> и Ce<sup>4+</sup>) на основу карактеристика спектралних структура добијених рендгенском спектрометријом. Утврђено је да узорак (I), формиран при 300 МПа и  $T = 1400$  °C у ваздуху, садржи на површини две врсте церијумових јона у атомском односу 63% Ce<sup>3+</sup> и 37% Ce<sup>4+</sup>, а да узорак (II), настао при 300 МПа и  $T = 1300$  °C у средини са кисеоником, садржи на својој површини такође две врсте церијумових јона, али у другом атомском односу – 36% Ce<sup>3+</sup> и 64% Ce<sup>4+</sup>. Установљено је да на површини проучаваних керамика под утицајем околине могу настати карбонати калцијума или церијума што води деструкцији саме керамике.